

# Development of novel PET probes, [ $^{18}\text{F}$ ]BCPP-EF, [ $^{18}\text{F}$ ]BCPP-BF, and [ $^{11}\text{C}$ ]BCPP-EM for mitochondrial complex 1 imaging in the living brain<sup>†</sup>

Norihiro Harada,\* Shingo Nishiyama, Masakatsu Kanazawa, and Hideo Tsukada

We developed three novel positron-emission tomography (PET) probes, 2-*tert*-butyl-4-chloro-5-{6-[2-(2-[ $^{18}\text{F}$ ]fluoroethoxy)ethoxy]-pyridin-3-ylmethoxy]-2H-pyridazin-3-one} ([ $^{18}\text{F}$ ]BCPP-EF), 2-*tert*-butyl-4-chloro-5-{6-(4-[ $^{18}\text{F}$ ]fluorobutoxy)-pyridin-3-ylmethoxy)-2H-pyridazin-3-one} ([ $^{18}\text{F}$ ]BCPP-BF), and 2-*tert*-butyl-4-chloro-5-{6-[2-(2-[ $^{11}\text{C}$ ]methoxy-ethoxy)-ethoxy]-pyridin-3-ylmethoxy)-2H-pyridazin-3-one} ([ $^{11}\text{C}$ ]BCPP-EM), for quantitative imaging of mitochondrial complex 1 (MC-1) activity *in vivo*. These three PET probes were successfully labeled by nucleophilic [ $^{18}\text{F}$ ]fluorination or by [ $^{11}\text{C}$ ]methylation of their corresponding precursor with sufficient radioactivity yield, good radiochemical purity, and sufficiently high specific radioactivity for PET measurement. The specificity of these probes for binding to MC-1 was assessed with rotenone, a specific MC-1 inhibitor, by a rat brain slice imaging method *in vitro*. Rat whole-body imaging by small-animal PET demonstrated that all probes showed high uptake levels in the brain as well as in the heart sufficient to image them clearly. The rank order of uptake levels in the brain and the heart just after injection was as follows: high in [ $^{18}\text{F}$ ]BCPP-BF, intermediate in [ $^{11}\text{C}$ ]BCPP-EM, and low in [ $^{18}\text{F}$ ]BCPP-EF. The kinetics of [ $^{18}\text{F}$ ]BCPP-EF and [ $^{11}\text{C}$ ]BCPP-EM provided a reversible binding pattern, whereas [ $^{18}\text{F}$ ]BCPP-BF showed nonreversible accumulation-type kinetics in the brain and heart. Metabolite analyses indicated that these three compounds were rapidly metabolized in the plasma but relatively stable in the rat brain up to 60 min post-injection. The present study demonstrated that [ $^{18}\text{F}$ ]BCPP-EF could be a useful PET probe for quantitative imaging of MC-1 activity in the living brain by PET.

**Keywords:** brain; PET; mitochondrial complex 1; [ $^{18}\text{F}$ ]BCPP-EF; [ $^{18}\text{F}$ ]BCPP-BF; [ $^{11}\text{C}$ ]BCPP-EM

## Introduction

The mitochondrial respiratory chain (complexes I-V) is the major site of ATP production in eukaryotic cells, and complex I (MC-1; NADH-ubiquinone oxidoreductase, EC 1.6.5.3) is the first enzyme of the respiratory electron transport chain and oxidative phosphorylation. MC-1 is critical for brain mitochondrial function, and its abnormalities have been observed in several neurodegenerative diseases such as Parkinson's disease (for review, see Shults<sup>1</sup>). A small loss in MC-1 activity is sufficient to decrease ATP synthesis and mitochondrial respiration in brain mitochondria and abolishes the threshold effect typically seen in normal cells subjected to oxidative stress. Thus, mitochondria are the main target of oxyradical-mediated damage. In parallel, because mitochondria are the main intracellular source of oxygen radical production,<sup>2</sup> ischemic insult may cause mitochondrial alterations when the oxygen concentration is re-established by reperfusion. When ischemic tissue is re-oxygenated, electron transport through the respiratory chain is impaired because of depletion of ADP during ischemia, and this leads to a burst of reactive oxygen species generation during the first minutes of reoxygenation.<sup>3</sup> Against this background, positron-emission tomography (PET) probes for imaging MC-1 function could be very useful for

diagnosing as well as monitoring the treatment efficacy of these neurodegenerative diseases.

The BMS-747158-01, a pyridazinone analog, showed inhibitory activity on MC-1 function by binding to the PSST subunit of MC-1, and its F-18 derivative [ $^{18}\text{F}$ ]BMS-747158-02 ([ $^{18}\text{F}$ ]BMS) was originally developed as a myocardial perfusion imaging agent.<sup>4,5</sup> It is noteworthy that whole-body PET imaging as well as tissue dissection method indicated relatively high uptake and long retention in the brain.<sup>5</sup> In our previous study in the rat brain by small-animal PET, we suggested that [ $^{18}\text{F}$ ]BMS might be useful to detect ischemic neuronal damage at acute and subacute phases after ischemic insult.<sup>6</sup> However, we also pointed out that [ $^{18}\text{F}$ ]BMS revealed relatively high nonspecific binding in the brain against inhibition with rotenone, a specific MC-1 inhibitor, in both *in vitro* and *in vivo* assessments.<sup>6</sup>

Central Research Laboratory, Hamamatsu Photonics K. K., Hamamatsu, Shizuoka 434-8601, Japan

\*Correspondence to: Norihiro Harada, Central Research Laboratory, Hamamatsu Photonics K.K., 5000 Hirakuchi, Hamakita, Shizuoka 434-8601, Japan.  
E-mail: norihiro@crl.hpk.co.jp

<sup>†</sup> Additional Supporting Information may be found in the on-line version of this article.

In the present study, three novel PET probes, 2-*tert*-butyl-4-chloro-5-[6-[2-( $^{18}\text{F}$ )fluoroethoxy]-ethoxy]-pyridin-3-ylmethoxy]-2H-pyridazin-3-one ( $^{18}\text{F}$ BCPP-EF), 2-*tert*-butyl-4-chloro-5-[6-(4-[ $^{18}\text{F}$ ]fluorobutoxy)-pyridin-3-ylmethoxy]-2H-pyridazin-3-one ( $^{18}\text{F}$ BCPP-BF), and 2-*tert*-butyl-4-chloro-5-[6-[2-(2-methoxyethoxy)-ethoxy]pyridin-3-ylmethoxy]-2H-pyridazin-3-one ( $^{11}\text{C}$ BCPP-EM), were designed, synthesized, and evaluated for their biodistribution in rats using small-animal PET with metabolite analyses in the plasma and brain. Furthermore, the binding specificity of  $^{18}\text{F}$ BCPP-EF,  $^{18}\text{F}$ BCPP-BF, and  $^{11}\text{C}$ BCPP-EM to MC-1 was assessed with rotenone, a specific MC-1 inhibitor, in rat living brain slice.

## Experimental

### Animals and chemicals

The following experiments were approved by the Ethical Committee of the Central Research Laboratory, Hamamatsu Photonics. Male Sprague–Dawley rats (Japan SLC, Hamamatsu, Japan) of 8 weeks of age (260–280 g) were used.

Chloral hydrate and rotenone were purchased from Wako Pure Chemical Industries, Ltd. (Osaka, Japan) and MP Biomedicals LLC (Santa Ana, CA, USA), respectively. Anhydrous  $\text{CH}_3\text{CN}$  was obtained from Sigma-Aldrich (St. Louis, MO, USA). Anion exchange resin AG1-X8 (OH- form, 100–200 mesh) was from Bio-Rad Laboratories (Hercules, CA, USA). Kryptofix222<sup>®</sup> (4,7,13,16,21,24-hexaoxa-1,10-diazabicyclo[8,8,8]hexacosane, K[2,2,2]), and  $\text{K}_2\text{CO}_3 \cdot 1.5\text{H}_2\text{O}$  were from Merck Millipore (Darmstadt, Germany). Silica gel (silica gel 60N, spherical neutral, 40–50  $\mu\text{m}$ , for flash chromatography) was from Kanto Chemical Co. Inc. (Tokyo, Japan). All other reagents and solvents were commercially available and used without further purification unless otherwise stated.

### Syntheses of precursors and standard compounds of $^{18}\text{F}$ BCPP-EF, $^{18}\text{F}$ BCPP-BF, and $^{11}\text{C}$ BCPP-EM

Nuclear magnetic resonance (NMR) spectra were recorded on an ECX-400P spectrometer (400 MHz, JEOL, Tokyo, Japan). High-resolution mass spectra (HRMS) were recorded on a QSTAR<sup>®</sup> Elite LC/MS/MS system (AB Sciex, Framingham, MA, USA).

#### Preparation of 2-*tert*-butyl-4-chloro-5-hydroxy-2H-pyridazin-3-one (1)

The 2-*tert*-Butyl-4,5-dichloro-2H-pyridazin-3-one was prepared according to a previous report.<sup>7</sup> A solution of 2-*tert*-butyl-4,5-dichloro-2H-pyridazin-3-one (2 g, 9 mmol) in 1,4-dioxane was supplemented with 0.1 g/mL aqueous KOH solution (15 mL, 27 mmol) and refluxed for 5 h. The reaction mixture was poured into iced  $\text{H}_2\text{O}$  and was neutralized with conc. HCl. Filtration of the precipitate and successive washing with  $\text{H}_2\text{O}$  and *n*-heptane gave **1** (1.6 g, 91%).  $^1\text{H-NMR}$  ( $\text{CD}_3\text{OD}$ ):  $\delta$  1.63 (s, 9H), 7.68 (s, 1H).

#### Synthesis of 2-chloro-5-(3-methyl-but-2-enyloxymethyl)-pyridine (2)

A solution of 6-chloro-3-pyridinemethanol (5 g, 34.8 mmol) in dimethylformamide (30 mL) was slowly added to NaH (60% in mineral oil, 1.51 g, 37.8 mmol) at  $0^\circ\text{C}$  under an argon atmosphere. The resulting solution was supplemented with 1-chloro-3-methyl-2-butene (4.11 mL, 36.5 mmol) and stirred for 1 h at  $25^\circ\text{C}$ . To consume the starting material, 1-chloro-3-methyl-2-butene (2.0 mL, 17.7 mmol) was added and stirred for another 1 h at  $50^\circ\text{C}$ . For complete consumption of the starting material, extra NaH (60% in mineral oil, 1.51 g, 37.8 mmol) and 1-chloro-3-methyl-2-butene (8.0 mL, 71.1 mmol) were added and stirred for 30 min at  $50^\circ\text{C}$ . The reaction mixture was supplemented with  $\text{H}_2\text{O}$  and extracted with EtOAc. Separated organic layer was washed with saturated NaCl, dried over anhydrous  $\text{Na}_2\text{SO}_4$ , and concentrated in vacuo. Chromatographic purification of the residue on silica gel (*n*-heptane/EtOAc = 95/5  $\rightarrow$  85/15) gave **2** (7.0 g, 96%) as a colorless oil.  $^1\text{H-NMR}$  ( $\text{CDCl}_3$ ):  $\delta$  1.67 (s, 3H), 1.76 (s, 3H), 4.01 (d, 1H,  $J = 6.8$  Hz), 4.11

(d, 1H,  $J = 6.8$  Hz), 4.48 (s, 2H), 5.37 (t, 1H,  $J = 6.8$  Hz), 7.30 (d, 1H,  $J = 8.4$  Hz), 7.66 (dd, 1H,  $J = 2.4$  and 8.4 Hz), 8.34 (d, 1H,  $J = 2.4$  Hz).

#### Preparation of 2-[2-(tetrahydro-pyran-2-yloxy)-ethoxy]-ethanol (3)

Diethylene glycol (22.8 mL, 0.24 mol) and 3,4-dihydro-2H-pyran (21.7 mL, 0.24 mol) were dissolved in a mixture of THF (40 mL) and  $\text{CH}_2\text{Cl}_2$  (400 mL). After cooling to  $-10^\circ\text{C}$ , *p*-toluenesulfonic acid monohydrate (4.57 g, 24 mmol) was added to the mixture and stirred for 1 h. The reaction mixture was supplemented with  $\text{H}_2\text{O}$  and extracted with  $\text{Et}_2\text{O}$ . The organic layer was washed with saturated NaCl, dried over anhydrous  $\text{Na}_2\text{SO}_4$ , and concentrated under reduced pressure. Chromatographic purification on silica gel (*n*-heptane/EtOAc = 1/1  $\rightarrow$  0/10) gave **3** (14 g, 31%) as a colorless oil.  $^1\text{H-NMR}$  ( $\text{CDCl}_3$ ):  $\delta$  1.28–1.65 (m, 4H), 1.70–1.77 (m, 1H), 1.80–1.87 (m, 1H), 2.54 (br, 1H), 3.49–3.54 (m, 1H), 3.60–3.66 (m, 3H), 3.70–3.74 (m, 4H), 3.85–3.91 (m, 2H), 4.64 (t, 1H,  $J = 4.0$  Hz).

#### Synthesis of 4-(tetrahydro-pyran-2-yloxy)-butan-1-ol (4)

Compound **4** was prepared by the same procedure as **3** from 1,4-butanediol (21.3 mL, 0.24 mol) instead of diethylene glycol. Chromatographic purification on silica gel (*n*-heptane/EtOAc = 1/1  $\rightarrow$  0/10) gave **4** (17 g, 41%) as a colorless oil.  $^1\text{H-NMR}$  ( $\text{CDCl}_3$ ):  $\delta$  1.51–1.63 (m, 4H), 1.65–1.76 (m, 4H), 1.79–1.85 (m, 2H), 3.41–3.46 (m, 1H), 3.49–3.54 (m, 1H), 4.67 (d, 2H,  $J = 5.6$  Hz), 4.59–4.61 (m, 1H).

#### Synthesis of 5-(3-methyl-but-2-enyloxymethyl)-2-[2-(tetrahydro-pyran-2-yloxy)ethoxy]-ethoxy-pyridine (5)

A solution of **3** (1.90 g, 10 mmol) in 1,4-dioxane (8 mL) was slowly added to NaH (60% in mineral oil, 0.32 g, 8 mmol) at  $0^\circ\text{C}$  under an argon atmosphere. The reaction mixture was stirred for 30 min at  $60^\circ\text{C}$  followed by the addition of **2** (0.84 g, 4 mmol) in 1,4-dioxane (4 mL). The reaction mixture was stirred for 30 min at  $170^\circ\text{C}$  with microwave heating. After cooling to room temperature, the reaction mixture was supplemented with saturated  $\text{NH}_4\text{Cl}$  solution and extracted with  $\text{CH}_2\text{Cl}_2$ . The organic layer was successively washed with  $\text{H}_2\text{O}$  and saturated NaCl, dried over anhydrous  $\text{MgSO}_4$ , and concentrated in vacuo. Chromatographic purification on silica gel (*n*-heptane/AcOEt = 95/5  $\rightarrow$  85/15) gave **5** (4.9 g, 96%).  $^1\text{H-NMR}$  ( $\text{CDCl}_3$ ):  $\delta$  1.28–1.82 (m, 12H), 3.49–3.59 (m, 1H), 3.60–3.74 (m, 3H), 3.85–3.89 (m, 4H), 3.97 (d, 2H,  $J = 6.8$  Hz), 4.40 (s, 2H), 4.46–4.48 (m, 2H), 4.64 (s, 1H), 5.38 (t, 1H,  $J = 7.2$  Hz), 6.76 (d, 1H,  $J = 8.4$  Hz), 7.58 (dd, 1H,  $J = 2.4$  and 8.4 Hz), 8.06 (d, 1H,  $J = 2.4$  Hz).

#### Synthesis of 5-(3-methyl-but-2-enyloxymethyl)-2-[4-(tetrahydro-pyran-2-yloxy)butoxy]-pyridine (6)

Compound **6** was synthesized by the same procedure as for **5** starting from **4** (0.43 g, 2.5 mmol). Chromatographic purification on silica gel (*n*-heptane/AcOEt = 99/1  $\rightarrow$  90/10) gave **6** (0.29 g, 84%).  $^1\text{H-NMR}$  ( $\text{CDCl}_3$ ):  $\delta$  1.54–1.89 (m, 16H), 3.42–3.526 (m, 2H), 3.77–3.86 (m, 2H), 3.98 (d, 2H,  $J = 7.2$  Hz), 4.31 (t, 2H,  $J = 6.8$  Hz), 4.40 (s, 2H), 4.59–4.60 (m, 1H), 5.35–5.38 (m, 1H), 6.70 (d, 1H,  $J = 9.2$  Hz), 7.58 (dd, 1H,  $J = 2.6$  and 8.6 Hz), 8.07 (d, 1H,  $J = 2.0$  Hz).

#### Synthesis of (6-[2-(tetrahydro-pyran-2-yloxy)-ethoxy]-ethoxy)-pyridin-3-ylmethanol (7)

Compound **5** (5 g, 13.6 mmol) was slowly added to a solution of *t*-BuOK (15.3 g, 0.13 mol) in DMSO (130 mL) under an argon atmosphere. The reaction mixture was stirred for 40 min at  $60^\circ\text{C}$ . After cooling to room temperature, the reaction mixture was supplemented with saturated aqueous  $\text{NH}_4\text{Cl}$  and extracted with EtOAc. The organic layer was successively washed with  $\text{H}_2\text{O}$  and saturated NaCl, dried over anhydrous  $\text{MgSO}_4$  followed by vacuum evaporation. The resulting residue was purified by silica gel column chromatography (*n*-heptane/EtOAc = 80/20) to give **7** (2.7 g, 68%) as a pale yellow oil.  $^1\text{H-NMR}$  ( $\text{CDCl}_3$ ):  $\delta$  1.52–1.83 (m, 6H), 3.49 (t, 1H,  $J = 5.6$  Hz), 3.60–3.65 (m, 1H), 3.72–3.74 (m, 2H), 3.84–3.90 (m, 4H), 4.46–4.48 (m, 2H), 4.61–4.64 (m, 3H), 6.77 (d, 1H,  $J = 4.0$  Hz), 7.58 (dd, 1H,  $J = 4.0$  Hz, 8.0 Hz), 8.08 (s, 1H).

### Synthesis of {6-[4-(tetrahydro-pyran-2-yloxy)-butoxy]-pyridin-3-yl}-methanol (**8**)

Compound **8** was synthesized by the same procedure as for **7** starting from **6** (3 g, 8.58 mmol). Chromatographic purification on silica gel (n-heptane/EtOAc=70/30 → 30/70) gave **8** (2.3 g, 94%) as a pale yellow oil. <sup>1</sup>H-NMR (CDCl<sub>3</sub>): δ 1.50–1.54 (m, 4H), 1.67–1.87 (m, 6H), 2.99 (br, 1H), 3.41–3.59 (m, 2H), 3.76–3.88 (m, 2H), 4.31 (t, 2H, J=6.8 Hz), 4.57 (s, 3H), 6.70 (d, 1H, J=8.8 Hz), 7.59 (dd, 1H, J=2.4 and 8.8 Hz), 8.04 (s, 1H).

### Synthesis of 2-tert-butyl-4-chloro-5-[6-[2-(2-(tetrahydro-pyran-2-yloxy)-ethoxy)ethoxy]-pyridin-3-ylmethoxy]-2H-pyridazin-3-one (**9**)

To a mixture of **1** (1.43 g, 7.04 mmol), **7** (2.3 g, 7.74 mmol), and PPh<sub>3</sub> (2.77 g, 10.6 mmol) in THF (100 mL) was added diisopropyl azodicarboxylate (2.09 mL, 10.6 mmol) under an argon atmosphere. After stirring for 16 h at 25°C, the reaction mixture was supplemented with H<sub>2</sub>O and extracted with EtOAc. The organic layer was washed with saturated NaCl, dried over anhydrous MgSO<sub>4</sub>, and concentrated under reduced pressure. Sequential purification by silica gel chromatography (heptane/EtOAc=90/10–60/40 then CHCl<sub>3</sub>/CH<sub>3</sub>OH=99/1) gave **9** (2.7 g, 80%). <sup>1</sup>H-NMR (CDCl<sub>3</sub>): δ 1.65 (9H, s), 1.52–1.83 (m, 15H), 3.48–3.50 (m, 1H), 3.60–3.66 (m, 1H), 3.72–3.75 (m, 2H), 3.84–3.91 (m, 4H), 4.48–4.51 (m, 2H), 4.64 (t, 1H, J=4.0 Hz), 5.22 (s, 2H), 6.84 (d, 1H, J=8.8 Hz), 7.65 (dd, 1H, J=2.4 and 8.8 Hz), 7.75 (s, 1H), 8.17 (d, 1H, J=2.4 Hz).

### Synthesis of 2-tert-butyl-4-chloro-5-[6-[4-(tetrahydro-pyran-2-yloxy)-butoxy]pyridin-3-ylmethoxy]-2H-pyridazin-3-one (**10**)

Compound **10** was prepared by the same procedure as for **9** starting from **8** (2.18 g, 7.74 mmol). Crude product was purified by silica gel chromatography (heptane/EtOAc=95/5 → 60/40) to give **10** (6.2 g, 84%). <sup>1</sup>H-NMR (CDCl<sub>3</sub>): δ 1.57 (s, 9H), 1.75 (dd, 2H, J=6.4, 14.4 Hz), 1.87 (dd, 2H, J=6.4, 14.4 Hz), 3.73 (t, 2H, J=6.4 Hz), 4.35 (t, 2H, J=6.4 Hz), 5.22 (s, 2H), 6.78 (d, 1H, J=8.8 Hz), 7.66 (dd, 1H, J=2.4, 8.8 Hz), 7.76 (s, 1H), 8.18 (d, 1H, J=2.4 Hz).

### Synthesis of 2-tert-butyl-4-chloro-5-[6-[2-(2-hydroxy-ethoxy)-ethoxy]-pyridin-3-ylmethoxy]-2H-pyridazin-3-one (**11**)

A mixture of **9** (96 mg, 7.2 mmol) and *p*-toluene sulfonic acid monohydrate (2 mg, 0.01 mmol) in CH<sub>3</sub>OH (1 mL) was stirred for 16 h at 25°C. After evaporation of the solvent under reduced pressure, chromatographic purification of the residue on silica gel (heptane/EtOAc=70/30 → 20/80) gave **11** (96.9 mg, 99%) as a colorless solid. <sup>1</sup>H-NMR (CDCl<sub>3</sub>): δ 1.64 (s, 9H), 3.65–3.67 (m, 2H), 3.75 (s, 1H), 3.87 (t, 2H, J=4.8 Hz), 4.51 (t, 2H, J=4.8 Hz), 5.22 (s, 2H), 6.85 (d, 1H, J=8.4 Hz), 7.67 (dd, 1H, J=2.0 and 8.4 Hz), 7.75 (s, 1H), 8.17 (d, 1H, J=2.0 Hz). Calcd for C<sub>18</sub>H<sub>25</sub>ClN<sub>3</sub>O<sub>5</sub> [(M+H)<sup>+</sup>] 398.1477, found 398.1493.

### Synthesis of 2-tert-butyl-4-chloro-5-[6-(4-hydroxy-butoxy)-pyridin-3-ylmethoxy]-2H-pyridazin-3-one (**12**)

Compound **12** was prepared by the same procedure as **11** from **10** (126 mg, 0.2 mmol). Chromatographic purification of crude product on silica gel (heptane/EtOAc=70/30 → 30/70) gave **12** (64 mg, 84%) as a colorless oil. <sup>1</sup>H-NMR (CDCl<sub>3</sub>): δ 1.57 (s, 9H), 1.75 (dd, 2H, J=6.4 and 14.4 Hz), 1.87 (dd, 2H, J=6.4 and 14.4 Hz), 3.73 (t, 2H, J=6.4 Hz), 4.35 (t, 2H, J=6.4 Hz), 5.22 (s, 2H), 6.78 (d, 1H, J=8.8 Hz), 7.66 (dd, 1H, J=2.4 and 8.8 Hz), 7.76 (s, 1H), 8.18 (d, 1H, J=2.4 Hz).

### Synthesis of toluene-4-sulfonic acid 2-[5-(1-tert-butyl-5-chloro-6-oxo-1,6-dihydro-pyridazin-4-yloxymethyl)-pyridin-2-yloxy]-ethoxy-ethyl ester (**13**)

A mixture of **11** (450 mg, 1.13 mmol), Et<sub>3</sub>N (1.58 mL, 11.3 mmol), and 4-dimethylamino-pyridine (13.8 mg, 0.11 mmol) in CH<sub>2</sub>Cl<sub>2</sub> (10 mL) was supplemented with *p*-toluenesulfonyl chloride (0.32 g, 1.69 mmol) below –10°C and then stirred for 16 h. H<sub>2</sub>O was added to the reaction mixture and extracted twice with CH<sub>2</sub>Cl<sub>2</sub>. The combined organic layer was washed with saturated NaCl, dried over anhydrous MgSO<sub>4</sub>, and concentrated in vacuo. Purification of the residue by silica gel column

chromatography (n-heptane/EtOAc, 90/10 → 40/60) gave **13** (610 mg, 97%). <sup>1</sup>H-NMR (CDCl<sub>3</sub>): δ 1.68 (s, 9H), 2.42 (s, 3H), 3.74 (t, 2H, J=4.8 Hz), 3.78 (t, 2H, J=4.8 Hz), 4.18 (t, 2H, J=4.8 Hz), 4.41 (t, 2H, J=4.8 Hz), 5.22 (s, 2H), 6.82 (d, 1H, J=8.8 Hz), 7.30 (d, 1H, J=8.0 Hz), 7.66 (dd, 1H, J=2.4 and 8.8 Hz), 7.76 (s, 1H), 7.79 (d, 2H, J=8.0 Hz), 8.18 (s, 1H). HRMS: Calcd for C<sub>25</sub>H<sub>31</sub>ClN<sub>3</sub>O<sub>7</sub>S [(M+H)<sup>+</sup>] 552.1565, found 552.1576.

### Synthesis of toluene-4-sulfonic acid 4-[5-(1-tert-butyl-5-chloro-6-oxo-1,6-dihydropyridazin-4-yloxymethyl)-pyridin-2-yloxy]-butyl ester (**14**)

Compound **14** was prepared by the same procedure as **13** from **12** (400 mg, 1.04 mmol). Purification of crude product by silica gel column chromatography (n-heptane/EtOAc, 95/5) gave **14** (458 mg, 82%). <sup>1</sup>H-NMR (CDCl<sub>3</sub>): δ 1.64 (s, 9H), 1.82 (t, 4H, J=2.8 Hz), 2.44 (s, 3H), 4.10 (s, 2H), 4.09–4.12 (m, 2H), 4.26 (d, 1H, J=6.0 Hz), 5.21 (s, 2H), 6.74 (d, 1H, J=8.4 Hz), 7.33 (d, 2H, J=7.6 Hz), 7.66 (dd, 1H, J=2.4 Hz, 8.8 Hz), 7.75 (s, 1H), 7.89 (d, 2H, J=8.8 Hz), 8.15 (s, 1H). HRMS: Calcd for C<sub>25</sub>H<sub>31</sub>ClN<sub>3</sub>O<sub>6</sub>S [(M+H)<sup>+</sup>] 536.1616, found 536.1626.

### Synthesis of 2-tert-butyl-4-chloro-5-[6-[2-(2-fluoro-ethoxy)-ethoxy]-pyridin-3-ylmethoxy]-2H-pyridazin-3-one (BCPP-EF)

Compound **13** (110 mg, 0.2 mmol) was added to 0.6 mL of TBAF (1.0 mol/L in THF, 0.6 mmol) and stirred for 16 h at 25°C. After evaporation of the solvent under reduced pressure, the residue was purified by silica gel chromatography (n-heptane/EtOAc=90/10 → 50/50) to give BCPP-EF (70 mg, 88%). <sup>1</sup>H-NMR (CDCl<sub>3</sub>): δ 1.64 (s, 9H), 3.77 (t, 1H, J=4.0 Hz), 3.84 (d, 1H, J=4.0 Hz), 3.89 (t, 2H, J=4.8 Hz), 4.51–4.54 (m, 3H), 4.65 (d, 1H, J=4.0 Hz), 5.22 (s, 2H), 6.85 (d, 1H, J=8.8 Hz), 7.65 (dd, 1H, J=2.4 Hz, 8.8 Hz), 7.75 (s, 1H), 8.17 (d, 1H, J=2.4 Hz). HRMS: Calcd for C<sub>18</sub>H<sub>24</sub>ClFN<sub>3</sub>O<sub>4</sub> [(M+H)<sup>+</sup>] 400.1433, found 400.1449.

### Synthesis of 2-tert-butyl-4-chloro-5-[6-(4-fluoro-butoxy)-pyridin-3-ylmethoxy]2H-pyridazin-3-one (BCPP-BF)

The BCPP-BF was prepared by the same procedure as BCPP-EF from **14** (70 mg, 0.13 mmol). Crude product was purified by silica gel chromatography (n-heptane/EtOAc=97/3 → 80/20) to give BCPP-BF (35 mg, 70%). <sup>1</sup>H-NMR (CDCl<sub>3</sub>): δ 1.64 (s, 9H), 1.81–1.94 (m, 4H), 4.35 (t, 2H, J=5.8 Hz), 4.46 (t, 1H, J=5.8 Hz), 4.58 (s, 1H), 5.22 (s, 2H), 6.72 (d, 1H, J=8.8 Hz), 7.66 (dd, 1H, J=2.6 and 8.8 Hz), 7.76 (s, 1H), 8.18 (s, 1H). HRMS: Calcd for C<sub>18</sub>H<sub>24</sub>ClFN<sub>3</sub>O<sub>3</sub> [(M+H)<sup>+</sup>] 384.1484, found 384.1500.

### Synthesis of 2-tert-butyl-4-chloro-5-[6-[2-(2-methoxy-ethoxy)-ethoxy]-pyridin-3-ylmethoxy]-2H-pyridazin-3-one (BCPP-EM)

In a sealed tube, a solution of **11** (80 mg, 0.2 mmol) in 1,4-dioxane (2 mL) was added to NaH (60% in mineral oil, 12 mg, 0.3 mmol) at 0°C under an argon atmosphere. 125 μL of CH<sub>3</sub>I (2 mmol) was added to the solution and stirred for 1 h at 25°C. After cooling to room temperature, H<sub>2</sub>O was added to the reaction mixture and extracted with EtOAc. Organic layer was washed with saturated NaCl and dried over MgSO<sub>4</sub>. Evaporation of the solvent under reduced pressure and purification by silica gel chromatography (n-heptane/EtOAc=70/30 → 30/70) gave BCPP-EM (62 mg, 75%). <sup>1</sup>H-NMR (CDCl<sub>3</sub>): δ 1.64 (s, 9H), 3.38 (s, 3H), 3.65–3.67 (m, 2H), 3.69–3.72 (m, 2H), 3.86 (t, 2H, J=4.8 Hz), 4.50 (t, 2H, J=4.8 Hz), 5.22 (s, 2H), 6.84 (d, 1H, J=8.8 Hz), 7.65 (dd, 1H, J=2.4 and 8.8 Hz), 7.75 (s, 1H), 8.16 (s, 1H). HRMS: Calcd for C<sub>19</sub>H<sub>27</sub>ClN<sub>3</sub>O<sub>5</sub> [(M+H)<sup>+</sup>] 412.1633, found 412.1649.

## Measurement of the distribution coefficient (log D<sub>7,4</sub>)

### BCPP-EF and BCPP-EM

CH<sub>3</sub>CN solution (500 μL) of BCPP-EF (750 μM) or BCPP-EM (534 μM) was dispensed into an Eppendorf pipette and evaporated. Each compound was dissolved in 1 mL of octanol, mixed with 1 mL of 0.1 M potassium phosphate buffer (pH 7.4), and vortexed for 5 min. After centrifugation at 12,000 rpm for 5 min, the two phases were separated. The octanol layer was diluted 10-fold with CH<sub>3</sub>CN, and the buffer layer was directly

injected onto the HPLC system for analysis of the concentration of the compound. The  $\log D_{7,4}$  was calculated from the log value of the concentration ratio of octanol to the buffer. Three separate determinations were carried out for each compound.

#### BCPP-BF

Approximately 3 mg of cold BCPP-BF was dissolved in 750  $\mu\text{L}$  of octanol, and the solution was dispensed into three vessels at 250  $\mu\text{L}$  each. Of 0.1 M potassium phosphate buffer (pH 7.4), 250  $\mu\text{L}$  was added to each solution, which was then vortexed for 5 min. After centrifugation at 12,000 rpm for 5 min, the two phases were separated. The octanol layer was diluted 10-fold with  $\text{CH}_3\text{CN}$ , and the buffer layer was directly injected onto the HPLC system for analysis of the concentration of the compound. The  $\log D_{7,4}$  was calculated from the log value of the concentration ratio of octanol to the buffer. Three separate determinations were carried out for each compound.

#### Radiolabeling of [ $^{18}\text{F}$ ]BCPP-EF, [ $^{18}\text{F}$ ]BCPP-BF, and [ $^{11}\text{C}$ ]BCPP-EM

Positron-emitting fluorine-18 ( $^{18}\text{F}$ ) and carbon-11 ( $^{11}\text{C}$ ) were produced by  $^{18}\text{O}(\text{p}, \text{n})^{18}\text{F}$  and  $^{14}\text{N}(\text{p}, \alpha)^{11}\text{C}$  nuclear reactions, respectively, using a cyclotron (HM-18, Sumitomo Heavy Industries, Ltd., Tokyo, Japan) at Hamamatsu Photonics PET Center. Labeled compounds were synthesized using a modified CUPID system (Sumitomo Heavy Industries, Ltd., Tokyo, Japan). HPLC analyses of labeled compounds were carried out on a GL-7400 low-pressure gradient HPLC system (GL Sciences, Inc., Tokyo, Japan) with a radioactivity detector (RLC-700, Hitachi Aloka Medical, Inc., Tokyo, Japan).

#### Synthesis of [ $^{18}\text{F}$ ]BCPP-EF

[ $^{18}\text{F}$ ]Fluoride was collected on ion-exchange resin AG1-X8 and eluted from the resin with 0.5 mL of 40 mM  $\text{K}_2\text{CO}_3 \cdot 1.5\text{H}_2\text{O}$ . To this fluoride solution,  $\text{K}[\text{2,2,2}]$  (15 mg) in  $\text{CH}_3\text{CN}$  (2 mL) was added. Water was removed by azeotropic distillation at 110°C under He flow. Addition of  $\text{CH}_3\text{CN}$  to the residue and azeotropic distillation were repeated twice. Then, the residue was dried under reduced pressure, and the reaction vessel was purged with He flow. Tosylate precursor **13** (10 mg) in  $\text{CH}_3\text{CN}$  (1 mL) was added to the dried [ $^{18}\text{F}$ ]KF/ $\text{K}[\text{2,2,2}]$  complex and reacted at 80°C for 10 min. After cooling the reaction mixture,  $\text{CH}_3\text{CN}/\text{H}_2\text{O}$  (=3/7) was added and transferred to an HPLC injector. Extra  $\text{CH}_3\text{CN}/\text{H}_2\text{O}$  (=3/7) was used to rinse the reaction vessel. Combined crude product was injected onto a semipreparative HPLC column (Inertsil ODS-3, GL Science, Tokyo, Japan) and eluted with  $\text{CH}_3\text{CN}/\text{H}_2\text{O}$  (=5/5). The radioactive peak at 17.5 min was collected and evaporated, and the residue was dissolved using saline with 0.1% Tween 80 and 1% ascorbic acid and recovered to a sterile vial. The final product was subjected to analytical HPLC with an analytical column (Finepak SIL C18S, JASCO corporation, Tokyo, Japan) with  $\text{CH}_3\text{CN}/30\text{ mM } \text{CH}_3\text{COONH}_4/\text{CH}_3\text{COOH}$  (=500/500/2). Total synthesis time was about 60 min from end of bombardment (EOB).

#### Synthesis of [ $^{18}\text{F}$ ]BCPP-BF

[ $^{18}\text{F}$ ]BCPP-BF was prepared following the same procedure as for [ $^{18}\text{F}$ ]BCPP-EF as described previously. In preparative HPLC, the radioactive peak at 35.1 min was collected. The final product was subjected to analytical HPLC with an analytical column (Finepak SIL C18S, JASCO Corporation, Tokyo, Japan) with  $\text{CH}_3\text{CN}/30\text{ mM } \text{CH}_3\text{COONH}_4/\text{CH}_3\text{COOH}$  (=500/500/2). Total synthesis time was about 80 min from EOB.

#### Synthesis of [ $^{11}\text{C}$ ]BCPP-EM

Cyclotron-produced [ $^{11}\text{C}$ ]CO<sub>2</sub> was trapped in a solution of  $\text{LiAlH}_4$  (0.5 mL, 0.1 M in THF, ABX Advanced Biochemical Compounds, Radeberg, Germany) with  $\text{N}_2$  flow at -20°C. After removal of solvent by  $\text{N}_2$  flow with heating, 0.5 mL of HI (57%, Nacalai Tesque, Kyoto, Japan) was added to the residue. Then, the resulting  $\text{CH}_3\text{I}$  was converted into [ $^{11}\text{C}$ ]  $\text{CH}_3\text{OTf}$  by passing through  $\text{AgOTf}$  (Sigma-Aldrich, St. Louis, MO, USA) packed in a quartz tube heated at 200°C.<sup>8</sup> The converted [ $^{11}\text{C}$ ]  $\text{CH}_3\text{OTf}$

was introduced to a solution of **11** (2 mg, 5  $\mu\text{mol}$ ) and NaH (60% in mineral oil, 2 mg, 125  $\mu\text{mol}$ , Nakalai Tesque, Kyoto, Japan) in acetone (0.3 mL, Wako Pure Chemicals Industries, Osaka, Japan) and reacted for 5 min at 40°C. The reaction mixture was transferred to an HPLC injector followed by rinsing with HPLC mobile phase ( $\text{CH}_3\text{CN}/30\text{ mM } \text{CH}_3\text{COONH}_4$  = 450/550). Combined crude product was injected onto a semipreparative HPLC column (Megapak SIL C18-10, JASCO Corporation, Tokyo, Japan) and eluted with  $\text{CH}_3\text{CN}/30\text{ mM } \text{CH}_3\text{COONH}_4$  (=450/550). The radioactive peak at 10.0 min was collected and evaporated, and the residue was dissolved using saline with 0.1% Tween 80 and 1% ascorbic acid and recovered to a sterile vial. The final product was subjected to analytical HPLC with an analytical column (Finepak SIL C18S, JASCO Corporation, Tokyo, Japan) with  $\text{CH}_3\text{CN}/30\text{ mM } \text{CH}_3\text{COONH}_4/\text{CH}_3\text{COOH}$  (=500/500/2). Total synthesis time was about 30 min from EOB.

#### Living brain slice imaging

The preparation methods of living brain slices followed a previous report.<sup>9</sup> Male Sprague-Dawley rats of 8 weeks of age were anesthetized using chloral hydrate (400 mg/kg, i.p.). After decapitation, the brains were quickly removed and immersed in ice-cold artificial cerebrospinal fluid (ACSF) (pH 7.4, 126 mM NaCl, 3.5 mM KCl, 1.25 mM  $\text{NaH}_2\text{PO}_4$ , 10 mM D-glucose, 2 mM  $\text{MgSO}_4$ , 24 mM HEPES, and 2 mM  $\text{CaCl}_2$ ). Brain slices of 300  $\mu\text{m}$  thickness were cut with a vibrating microtome (MICROM HM650V, Thermo Fisher Scientific Inc., Waltham, MA, USA), and the slices were pre-incubated in 25 mL of ACSF followed by bubbling of 100% O<sub>2</sub> gas for 30 min at room temperature. The vehicle or rotenone with a final concentration of 2, 20, 200, or 2000 nM was added to the incubation ACSF solution and incubated for 30 min. For the determination of nonspecific binding, 20  $\mu\text{M}$  rotenone was used for incubation. Then, 40 MBq/mL of each probe was added to the incubation ACSF solution, followed by additional 30-min incubation. After washing with ACSF for 30 min at room temperature, the slices were transferred to a phosphoimaging plate (BAS-III, Fuji Film, Tokyo, Japan) for 10 min of exposure with an authentic standard radioactivity source. Radioactivity was converted to digitalized imaging data using a Fuji BAS system (FLA-7000, Fuji Film, Tokyo, Japan). Specific binding of [ $^{18}\text{F}$ ]BCPP-EF, [ $^{18}\text{F}$ ]BCPP-BF, or [ $^{11}\text{C}$ ]BCPP-EM to MC-1 at each rotenone concentration was calculated by subtraction of the radioactivity of nonspecific binding determined at 20  $\mu\text{M}$  from the radioactivity at each dose of rotenone.

#### Positron-emission tomography imaging

The PET scans were conducted with a high-resolution small-animal PET scanner (ClairvivoPET, Shimadzu Corporation, Kyoto, Japan)<sup>10</sup> with a resolution of 1.5 mm full width at half maximum. Four animals per group were used for PET imaging. Rats anesthetized by initial dosing with chloral hydrate (400 mg/kg, i.p.) followed by continuous infusion of chloral hydrate (100 mg/kg/h, i.v.) were positioned prone on a fixation plate and placed in the gantry hole of the PET scanner. After transmission measurement with an external  $^{137}\text{Cs}$  point source (22 MBq) for attenuation correction, PET ligand at ca. 8 MBq for [ $^{18}\text{F}$ ]BCPP-EF and [ $^{18}\text{F}$ ]BCPP-BF, or 20 MBq for [ $^{11}\text{C}$ ]BCPP-EM was intravenously injected into each rat from the tail vein. The data were acquired in list-mode format for 60 min; full 3-D sinograms with corrected efficiency, scattering, attenuation, count losses, and decay were reconstructed using an iterative 3-D dynamic raw-action maximum likelihood algorithm.<sup>11</sup> Dynamic images as well as summation images from 10 min to 30 min after the injection were reconstructed, and standard uptake value (SUV) images were created as the radioactivity in each pixel divided by the ratio of the total injected radioactivity and body weight. Each SUV image was superimposed on the corresponding X-ray CT computed tomography images obtained using a Clairvivo CT (Shimadzu Corporation, Kyoto, Japan). Regions of interest were placed on PET images of the myocardial region of the heart, and of the cortical region of the brain with the aid of a rat brain atlas<sup>12</sup>

## Metabolite analyses

For plasma metabolite analyses, the blood samples, obtained at 1, 5, 10, 30, and 60 min after the injection of each ligand, were centrifuged to separate plasma and weighed, and their radioactivity was measured. EtOH was added to plasma samples (sample/EtOH = 1/1), followed by centrifugation. The obtained supernatants were developed with thin layer chromatography plates (AL SIL G/UV, Whatman, Kent, UK) with a mobile phase of EtOAc. The ratio of unmetabolized fraction was determined using a phosphoimaging plate (FLA-7000, Fuji Film, Tokyo, Japan). The ratios of unmetabolized [ $^{18}\text{F}$ ]BCPP-EF, [ $^{18}\text{F}$ ]BCPP-BF, and [ $^{11}\text{C}$ ]BCPP-EM were calculated using the data obtained by correction of the ratio of the unmetabolized fraction to total radioactivity.

For brain metabolite analyses, the brain samples obtained at 5, 30, and 60 min after the injection of each ligand were minced, added ice cooled EtOH (2.0 mL), and homogenized (Polytron PT300, Kinematica AG, Littau, Switzerland) for 30 s. Aliquots of homogenate (0.4 mL) were transferred to eppendorf tube and centrifuged. Resulting supernatants were separated and analyzed in the same manner as plasma sample.

## Results and discussion

For designing novel PET probes for MC-1 imaging by PET, we hypothesized that relatively high nonspecific binding of [ $^{18}\text{F}$ ]BMS in the brain derived from its high lipophilicity. Thus, we intended to design PET probes with lower nonspecific binding by reducing their lipophilicity. Because 2-*tert*-butyl-4-chloro-2H-pyridazin-3-one moiety was reported to be important for affinity to MC-1,<sup>13</sup> the replacement of 1,4-dihydroxymethyl-benzene with 5-hydroxymethyl-2-hydroxy-pyridine and extension of one ethylene glycol unit on a side chain led to [ $^{18}\text{F}$ ]BCPP-EF and [ $^{11}\text{C}$ ]BCPP-EM structures. To prove our hypothesis, a saturated alkyl analog [ $^{18}\text{F}$ ]BCPP-BF with higher lipophilicity was also designed.

The processes of syntheses of the precursors and standard compounds are shown in Figure 1. Introduction of a side chain

was accomplished by etherification of hydroxyl-protected chloropyridine methanol (**2**) with monoprotected diol under microwave heating. After deprotection by *t*-BuOK, key compounds **11** and **12** were obtained by Mitsunobu coupling of pyridazinone and acid hydrolysis. Tosylation of **11** and **12** gave precursors **13** and **14**, respectively. Standard compounds of BCPP-EF and BCPP-BF were synthesized by fluorination of corresponding tosylate precursors, and BCPP-EM was synthesized by the methylation of **11**.

The assessment of lipophilicity of these three probes indicated that the distribution coefficient ( $\log D_{7.4}$ ) values of cold BCPP-BF, BCPP-EF, and BCPP-EM were 4.27, 3.03, and 2.87, respectively.

Radiosyntheses of [ $^{18}\text{F}$ ]BCPP-EF, [ $^{18}\text{F}$ ]BCPP-BF, and [ $^{11}\text{C}$ ]BCPP-EM were conducted as shown in the scheme of Figure 2. HPLC analytic charts demonstrated that the retention times for [ $^{18}\text{F}$ ]BCPP-EF, [ $^{18}\text{F}$ ]BCPP-BF, and [ $^{11}\text{C}$ ]BCPP-EM were 4.6, 8.3, and 4.0 min, respectively, which were identical to the corresponding authentic standard compounds (Figure 3). As shown in Table 1, these three novel PET probes were successfully labeled by nucleophilic [ $^{18}\text{F}$ ]fluorination or by [ $^{11}\text{C}$ ]methylation of their corresponding precursor with sufficient radioactivity yield ( $5.1 \pm 0.9$ ,  $3.7 \pm 1.1$ , and  $1.4 \pm 0.5$  GBq) (mean  $\pm$  SD,  $n = 5$ ), good radiochemical purity ( $99.1 \pm 0.7$ ,  $99.6 \pm 0.6$ , and  $98.4 \pm 1.8\%$ ), and sufficiently high specific radioactivity ( $139.6 \pm 37.0$ ,  $111.8 \pm 40.1$ , and  $332.0 \pm 228.5$  GBq/ $\mu\text{mol}$ ) for [ $^{18}\text{F}$ ]BCPP-EF, [ $^{18}\text{F}$ ]BCPP-BF, and [ $^{11}\text{C}$ ]BCPP-EM, respectively, by 1-h irradiation at 20  $\mu\text{A}$ . Among these three probes, the labeling of [ $^{11}\text{C}$ ]BCPP-EM seemed relatively unstable compared with those of the other two [ $^{18}\text{F}$ ]labeled probes (Table 1). We found several large peaks other than precursor in the preparative HPLC chromatogram (Supporting Information). The formation of these peaks suggests that decomposition of precursor and/or product occurred under strongly basic reaction condition. The decomposition was probably the cause of lower radiochemical yield of [ $^{11}\text{C}$ ]BCPP-EM.

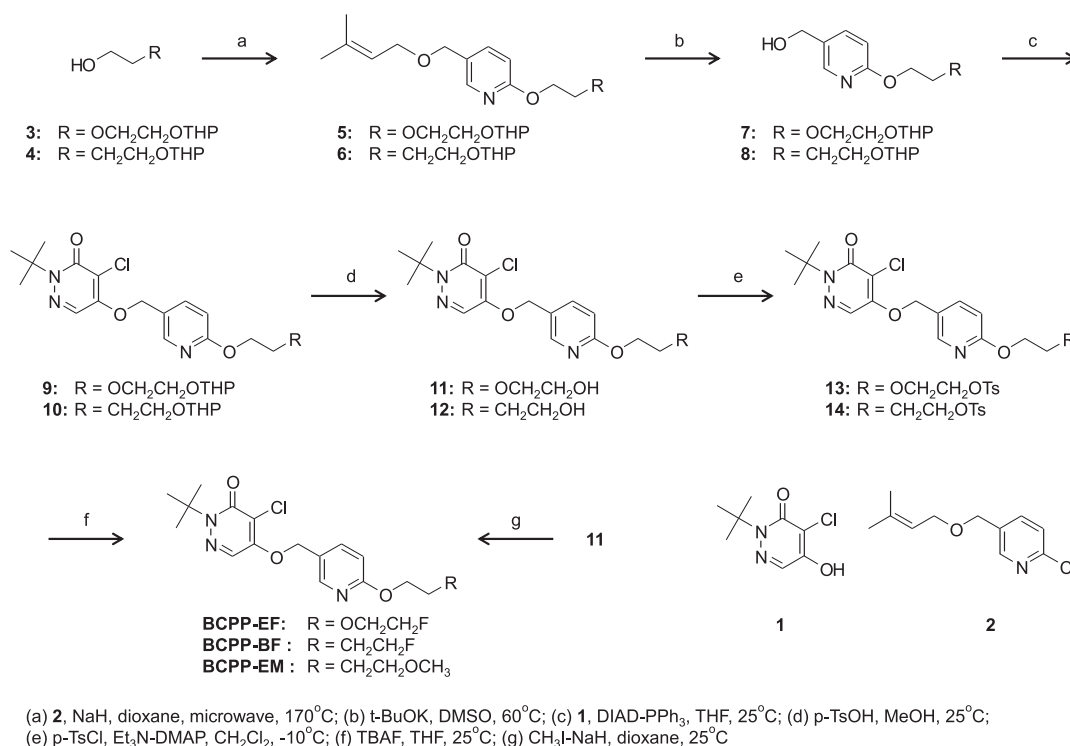


**Figure 1.** Syntheses of precursors and standard compounds of [ $^{18}\text{F}$ ]BCPP-EF, [ $^{18}\text{F}$ ]BCPP-BF, and [ $^{11}\text{C}$ ]BCPP-EM.

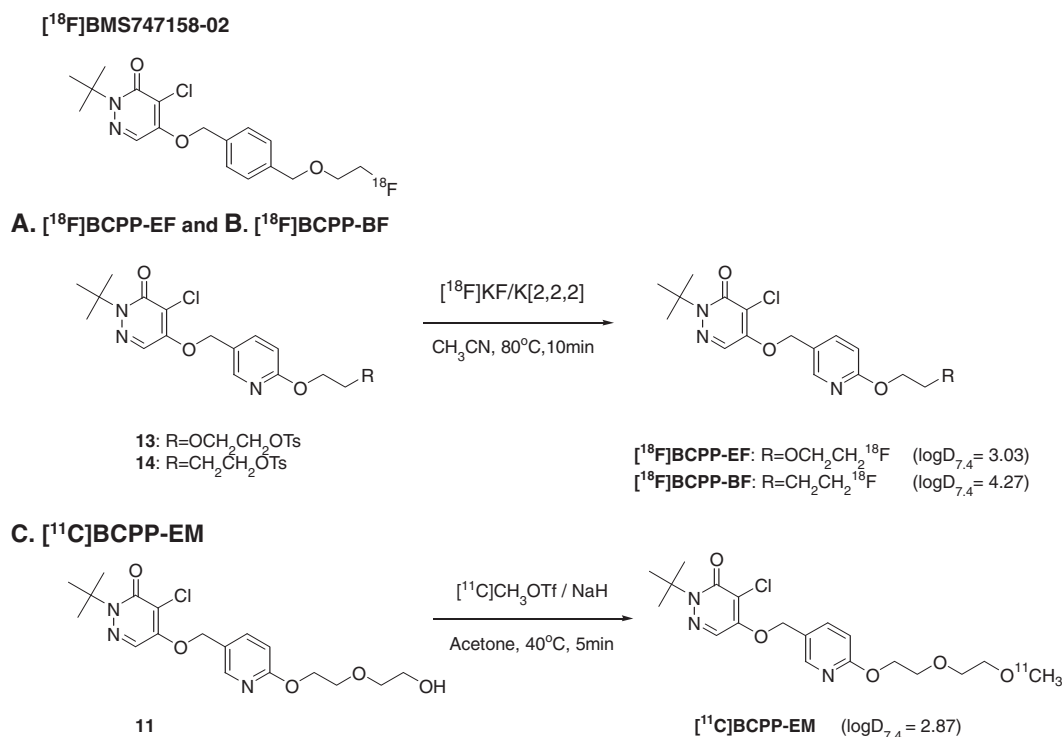


**Figure 2.** Radiolabeling of [<sup>18</sup>F]BCPP-EF (A), [<sup>18</sup>F]BCPP-BF (B), and [<sup>11</sup>C]BCPP-EM (C).

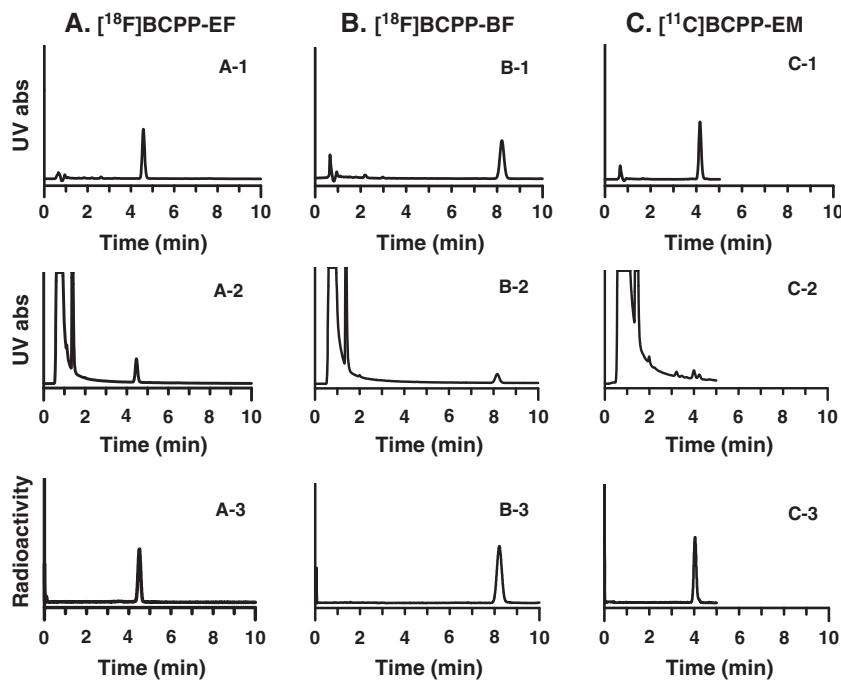


**Figure 3.** HPLC analyses of [<sup>18</sup>F]BCPP-EF (A), [<sup>18</sup>F]BCPP-BF (B), and [<sup>11</sup>C]BCPP-EM (C). The authentic standard compounds were analyzed by ultraviolet detection with corresponding HPLC systems to determine the retention times for BCPP-EF (A-1), BCPP-BF (B-1), and BCPP-EM (C-1). Then, the final products of radiolabeling were analyzed by ultraviolet (A-2, B-2, and C-2) and radioactivity (A-3, B-3, and C-3) detections with the same HPLC systems for identification and determination of the radiochemical purities of these probes.

For the assessments of the specificity in the binding of [<sup>18</sup>F]BCPP-EF (Figure 4(A and D)), [<sup>18</sup>F]BCPP-BF (Figure 4(B and D)), and [<sup>11</sup>C]BCPP-EM (Figure 4(C and D)) to MC-1, the *in vitro* binding properties were assessed with rotenone, a specific MC-1 inhibitor, *in vitro* using rat living brain slices. The binding

of these probes to brain slices was decreased by competitive inhibition with pre-incubated rotenone in a dose-dependent manner (Figure 4(A–D)). The nonspecific binding ratios of [<sup>18</sup>F]BCPP-EF (ca. 4%) and [<sup>11</sup>C]BCPP-EM (ca. 2%) assessed with rotenone at 20 μM were significantly lower than that of

<b>Table 1.</b> Radiosyntheses of [ $^{18}\text{F}$ ]BCPP-EF, [ $^{18}\text{F}$ ]BCPP-BF, and [ $^{11}\text{C}$ ]BCPP-EM				
	Yield (GBq)	Radiochemical Yield (%)	Radiochemical Purity (%)	Specific radioactivity (GBq/ $\mu\text{mol}$ )
[ $^{18}\text{F}$ ]BCPP-EF	5.1 $\pm$ 0.9	30.8 $\pm$ 4.2	99.1 $\pm$ 0.7	139.6 $\pm$ 37.0
[ $^{18}\text{F}$ ]BCPP-BF	3.7 $\pm$ 1.1	16.3 $\pm$ 2.7	99.6 $\pm$ 0.6	111.8 $\pm$ 40.1
[ $^{11}\text{C}$ ]BCPP-EM	1.4 $\pm$ 0.5	8.6 $\pm$ 0.8	98.4 $\pm$ 1.8	332.0 $\pm$ 228.5

Each radiosynthesis was conducted after 60 min irradiation for F-18/C-11 productions in a cyclotron. Data are expressed as mean  $\pm$  SD for five syntheses for each probe.

[ $^{18}\text{F}$ ]BCPP-BF (ca. 34%), and also the rotenone-induced degrees of reduction of [ $^{18}\text{F}$ ]BCPP-EF and [ $^{11}\text{C}$ ]BCPP-EM at each dose were more remarkable than those of [ $^{18}\text{F}$ ]BCPP-BF (Figure 4(A–D)).

The biodistributions of [ $^{18}\text{F}$ ]BCPP-EF, [ $^{18}\text{F}$ ]BCPP-BF, and [ $^{11}\text{C}$ ]BCPP-EM were preliminarily evaluated by small-animal PET in rats. The PET imaging with [ $^{18}\text{F}$ ]BCPP-EF (Figure 5A), [ $^{18}\text{F}$ ]BCPP-BF (Figure 5B), and [ $^{11}\text{C}$ ]BCPP-EM (Figure 5C) revealed the relatively high uptake of these three probes in the heart (SUV = 10.2, 8.6, and 9.4, respectively, at 30 min post-injection) and brain (SUV = 2.9, 2.0, and 2.4 in the cortex, respectively, at 30 min post-injection) of rat.

Analyses of time–activity curves indicated that the brain kinetics of [ $^{18}\text{F}$ ]BCPP-EF and [ $^{11}\text{C}$ ]BCPP-EM revealed rapid uptake after the injection, followed by gradual elimination (Figure 6(A-1 and C-1)), whereas that of [ $^{18}\text{F}$ ]BCPP-BF showed rapid uptake to a constant level up to 60 min after the injection (Figure 6B-1). In heart, [ $^{18}\text{F}$ ]BCPP-EF and [ $^{11}\text{C}$ ]BCPP-EM showed rapid uptake to a constant level up to 30 min after injection, followed by decline thereafter (Figure 6A-1 and C-1), whereas the uptake of [ $^{18}\text{F}$ ]BCPP-BF continuously increased with time (Figure 6B-1).

Plasma metabolite analyses of [ $^{18}\text{F}$ ]BCPP-EF (Figure 6A-2), [ $^{11}\text{C}$ ]BCPP-EM (Figure 6B-2), and [ $^{11}\text{C}$ ]BCPP-EM (Figure 6C-2) revealed the gradual degradation to polar metabolites with relatively slow rate, remaining 17.3%, 18.4%, and 25.5%, respectively, as the corresponding parent compounds 30 min after the injection. In contrast, the metabolite analyses of these three compounds in the brain demonstrated that they were all relatively stable in the brain tissues up to 60 min after the injection into rats, showing 90.4%, 97.1%, and 96.1%, respectively, 30 min after the injection (Fig. 6(A-2, B-2, and C-2)). Because species-specific differences in metabolism in plasma and brain should be taken into account, we must analyze the metabolic profiles of these PET probes in monkey before proceeding to clinical PET study.

The present study firstly evaluated the usefulness of [ $^{18}\text{F}$ ]BCPP-EF, [ $^{18}\text{F}$ ]BCPP-BF, and [ $^{11}\text{C}$ ]BCPP-EM as PET probes for imaging MC-1 activity in living rat brain by PET. It has been proposed that an ideal PET probe should have high and rapid uptake, rapid extraction from nontarget regions, and reasonable retention in the target regions. From these perspectives, the present study suggested that [ $^{18}\text{F}$ ]BCPP-EF could be one of the best probe for the quantitative imaging of cortical MC-1 among them. It was expected that, if the brain uptake was exclusively lipophilicity

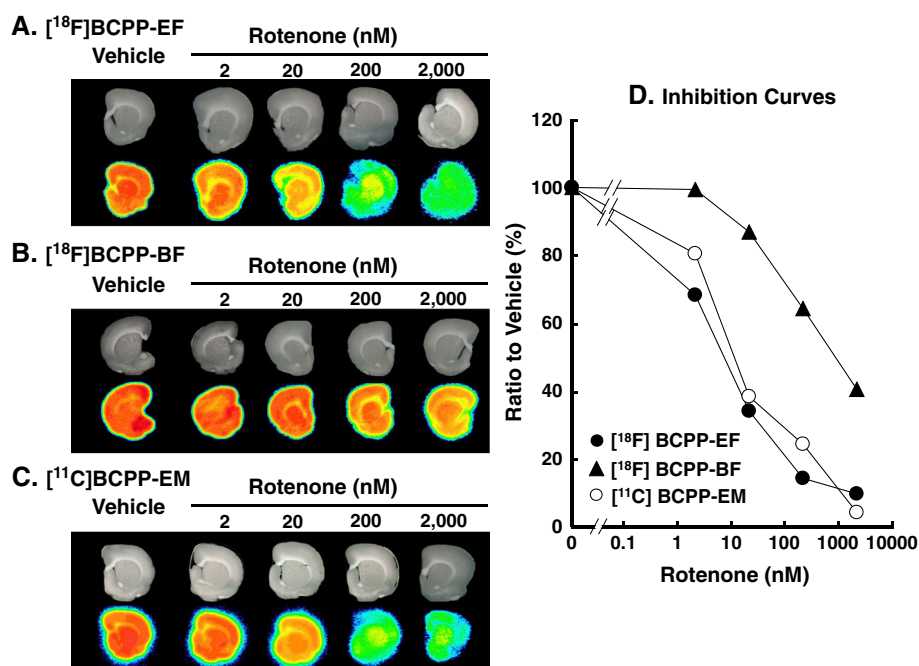


**Figure 4.** Effects of rotenone on binding of [ $^{18}\text{F}$ ]BCPP-EF, [ $^{18}\text{F}$ ]BCPP-BF, and [ $^{11}\text{C}$ ]BCPP-EM to rat living rat brain slice. Living brain slices dissected from rat were pre-incubated for 30 min at room temperature with vehicle or rotenone at doses of 2, 20, 200, and 2,000 nM, and then each probe was added to the incubation vessel and incubated for 30 min.

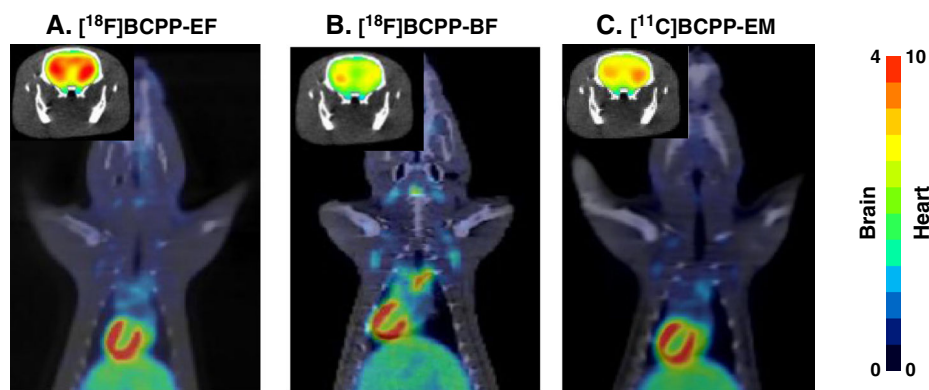


**Figure 5.** Positron-emission tomography images of [ $^{18}\text{F}$ ]BCPP-EF (A), [ $^{18}\text{F}$ ]BCPP-BF (B), and [ $^{11}\text{C}$ ]BCPP-EM (C) in rats. PET scanning was conducted for 60 min after injection of [ $^{18}\text{F}$ ]BCPP-EF, [ $^{18}\text{F}$ ]BCPP-BF, and [ $^{11}\text{C}$ ]BCPP-EM, and then summation data from 10 min to 30 min were reconstructed for standard uptake value images.

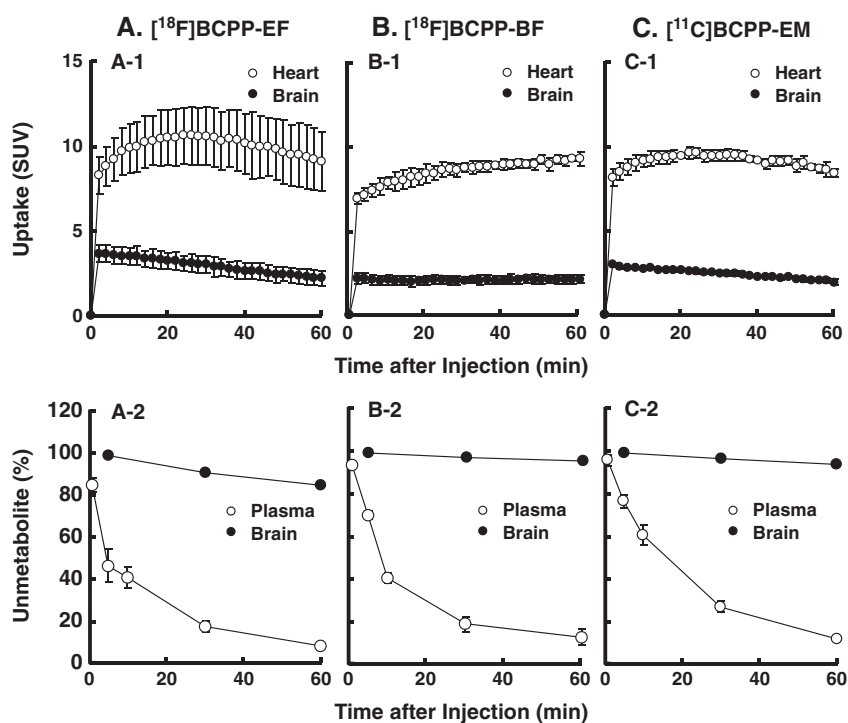


**Figure 6.** Time-activity curves of [ $^{18}\text{F}$ ]BCPP-EF (A), [ $^{18}\text{F}$ ]BCPP-BF (B), and [ $^{11}\text{C}$ ]BCPP-EM (C) in the brain and heart (A-1, B-1, and C-1) and their metabolite analyses in the brain and plasma of rat (A-2, B-2, and C-2). Regions of interest for the brain (cortex) and heart (myocardium) were set on each PET image reconstructed as described in Figure 5 legend to obtain time-activity curves of each probe (A-1, B-1, and C-1). Brain and plasma samples were obtained at several time points after the injection of each probe, then metabolite analyses was conducted to measure the unmetabolized fraction ratio at each time.

( $\log D_{7,4}$ )-driven, the rank order of brain uptake should be as follows: high in [ $^{18}\text{F}$ ]BCPP-BF (4.27), intermediate in [ $^{18}\text{F}$ ]BCPP-EF (3.03), and low in [ $^{11}\text{C}$ ]BCPP-EM (2.87). However, the rank order of uptake levels in the brain and heart just after the injection were high in [ $^{18}\text{F}$ ]BCPP-BF, intermediate in [ $^{11}\text{C}$ ]BCPP-EM, and low in [ $^{18}\text{F}$ ]BCPP-EF, which did not reflect the rank order of their  $\log D_{7,4}$  values. Modeling of the transport mechanisms of these compounds needs to take into account more complex systems including plasma protein binding ratios, which are affected by the lipophilicity of probes.

The kinetics of [ $^{18}\text{F}$ ]BCPP-EF and [ $^{11}\text{C}$ ]BCPP-EM in brain as well as heart provided a reversible binding pattern. In contrast,

[ $^{18}\text{F}$ ]BCPP-BF showed nonreversible and accumulation-type kinetics in the brain and heart. When considering the different kinetic patterns, the issues of affinity to MC-1 and lipophilicity should be taken into account. The *in vitro* assessments using living brain slices indicated that, although all three probes developed here showed specificity to MC-1, the  $\text{IC}_{50}$  value of [ $^{18}\text{F}$ ]BCPP-BF against rotenone was higher than those of [ $^{18}\text{F}$ ]BCPP-EF and [ $^{11}\text{C}$ ]BCPP-EM. The assessed  $\log D_{7,4}$  values of [ $^{18}\text{F}$ ]BCPP-BF (4.27), [ $^{18}\text{F}$ ]BCPP-EF (3.03), and [ $^{11}\text{C}$ ]BCPP-EM (2.87) resulted in higher nonspecific binding ratios of [ $^{18}\text{F}$ ]BCPP-BF than those of [ $^{18}\text{F}$ ]BCPP-EF and [ $^{11}\text{C}$ ]BCPP-EM. Although these two different factors might have caused the

different properties among these three probes, further evaluation is needed, such as on the stability in plasma and on the *in vivo* specificity/sensitivity against rotenone loading.

## Conclusion

In the present study, we succeeded in developing three novel PET probes, [ $^{18}\text{F}$ ]BCPP-EF, [ $^{18}\text{F}$ ]BCPP-BF, and [ $^{11}\text{C}$ ]BCPP-EM, for MC-1 imaging, and the preliminary evaluations demonstrated that [ $^{18}\text{F}$ ]BCPP-EF could be very useful as a PET probe for quantitative imaging of MC-1 activity in the living brain by PET.

## Acknowledgements

We are grateful for the technical assistance provided by Dai Fukumoto and Teruyo Hosoya.

## Conflict of Interest

The authors did not report any conflict of interest.

## References

- [1] C. W. Shults, *Mitochondrion* **2004**, *4*, 641–648.
- [2] E. Cadenas, A. Boveris, C. I. Ragan, A. O. Stoppani, *Arch. Biochem. Biophys.* **1977**, *180*, 248–257.
- [3] J. L. Zweier, J. T. Flaherty, M. L. Weisfeldt, *Proc. Natl. Acad. Sci. U.S.A.* **1987**, *84*, 1404–1407.
- [4] T. Higuchi, S. G. Nekolla, M. M. Huisman, S. Reeder, T. Poethko, M. Yu, H.-J. Wester, D. S. Casebier, S. P. Robinson, R. M. Botnar, *et al.*, *J. Nucl. Med.* **2008**, *49*, 1715–1722.
- [5] P. Yalamanchili, E. Wexler, M. Hayes, M. Yu, J. Bozek, M. Kagan, H. S. Radeke, M. Azure, A. Purohit, D. S. Casebier, *et al.*, *J. Nucl. Cardiol.* **2007**, *14*, 782–788.
- [6] D. Fukumoto, S. Nishiyama, N. Harada, S. Yamamoto, H. Tsukada, *Synapse* **2012**, *66*, 909–917.
- [7] B. Latli, H. Morimoto, P. G. Williams, J. E. Casida, *J. Label. Compd. Radiopharm.* **1998**, *41*, 191–199.
- [8] D. M. Jewett, *Appl. Radiat. Isot.* **1992**, *43*, 1383–1385.
- [9] K. Matsumura, M. Bergström, H. Onoe, H. Takechi, G. Westerberg, G. Antoni, P. Bjurling, G. B. Jacobson, B. Långström, Y. Watanabe, *Neurosci. Res.* **1995**, *22*, 219–229.
- [10] T. Mizuta, K. Kitamura, H. Iwata, Y. Yamagishi, A. Ohtani, K. Tanaka, Y. Inoue, *Ann. Nucl. Med.* **2008**, *22*, 447–455.
- [11] E. Tanaka, H. Kudo, *Phys. Med. Biol.* **2003**, *48*, 1405–1422.
- [12] G. Paxinos, C. Watson, *The Rat Brain in Stereotaxic Coordinates*, Academic Press/Elsevier, Amsterdam, **2007**.
- [13] A. Purohit, H. Radeke, M. Azure, K. Hanson, R. Benetti, F. Su, P. Yalamanchili, M. Yu, M. Hayes, M. Guaraldi, *et al.*, *J. Med. Chem.* **2008**, *51*, 2954–2970.